frontiers in Oncology

ORIGINAL RESEARCH
published: 02 November 2020
doi: 10.3389/fonc.2020.01688

EGFR/FOXO3A/LXR-α Axis Promotes Prostate Cancer Proliferation and Metastasis and Dual-Targeting LXR-α/EGFR Shows Synthetic Lethality

Tingting Chen, Jie Xu and Weihua Fu**

Department of Urology, The Second Affiliated Hospital, Third Military Medical University (Army Medical University), Chongqing, China

Prostate cancer is the second leading cause of cancer-related death in men. Early prostate cancer has a high 5-year survival rate. However, the five-year survival rate is low in progressive prostate cancer, which manifests as bone metastasis. The EGF receptor overexpression increases during disease progression and in the development of castration-resistant disease, and may be a potential therapeutic target. Liver X receptors (LXRs) are ligand-dependent nuclear receptor transcription factors and consist of two subtypes, LXR-α and LXR-β, which can inhibit tumor growth in various cancer cells. We revealed that LXR-α, but not LXR-β, was reduced in prostate cancer tissues compared with adjacent normal tissues. LXRs' agonist GW3965 enhanced the inhibitory action of LXR-α on the proliferation and metastasis of prostate cancer cells. Furthermore, our results support the notion that LXR-α is regulated by the EGFR/AKT/FOXO3A pathway. As an EGFR inhibitor, Afatinib could weaken AKT activation and increase the expression level of FOXO3A in prostate cancer. In addition, we indicated that the combination of Afatinib and GW3965 simultaneously increased and activated LXR-α, which led to an increase of tumor suppressors, and eventually inhibited tumor progression. Therefore, the combination of EGFR inhibitor and LXRs agonist may become a potential treatment strategy for prostate cancer, especially metastatic prostate cancer.

Keywords: prostate cancer, EGFR, FoxO3a, LXR-α, proliferation, metastasis

OPEN ACCESS

Edited by:
George Kulik,
Wake Forest University, United States

Reviewed by:
Rafael Rosell,
Catalan Institute of Oncology, Spain
Carmine D'Aniello,
AORN – Ospedali dei Colli, Italy

****Correspondence:***
Weihua Fu
fuweihua80@tmmu.edu.cn
Jie Xu
xujie1981@tmmu.edu.cn

Specialty section:
This article was submitted to Genitourinary Oncology, a section of the journal Frontiers in Oncology

Received: *26 May 2020*
Accepted: *29 July 2020*
Published: *02 November 2020*

Citation:
Chen T, Xu J and Fu W (2020) EGFR/FOXO3A/LXR-α Axis Promotes Prostate Cancer Proliferation and Metastasis and Dual-Targeting LXR-α/EGFR Shows Synthetic Lethality. Front. Oncol. 10:1688. doi: 10.3389/fonc.2020.01688

INTRODUCTION

Prostate cancer is the second leading cause of cancer-related death in men (1). In China, prostate cancer leads to 25,000 deaths annually, and the estimated 5-year survival rate is 54% (2, 3). Androgen receptor (AR), the first effector of testosterone action, activates certain genes involved in tumor growth and metastasis (4). Systemic therapy for advanced prostate cancer has largely focused on targeting AR. Thus, androgen deprivation therapy (ADT) is the main treatment for metastatic prostate cancer (5, 6). Unfortunately, remissions are temporary because surviving prostate cancer cells adapt to the androgen-deprived environment to form castration-resistant prostate cancer (CRPC) (7, 8). The acquisition of androgen independence may be due to the up-regulation of growth factor/receptor signaling pathways, such as the epidermal growth factor receptor (EGFR) signaling pathway (9, 10).

EGFR interacts with its ligand EGF, which leads to the activation of several downstream intracellular signaling pathways, including MEK, ERK and PI3K/AKT, and STAT3 (11). EGFR reduces tumor suppressors and activates oncogenes to promote prostate cancer progression and bone metastasis (12, 13). The expression of EGFR is correlated with the risk of recurrence and progression to hormone resistance (14). Many studies indicate that EGFR is a potential therapeutic target for prostate cancer, especially for patients with CRPC. However, some clinical trials using EGFR inhibitors alone have not found significant therapeutic effects. Afatinib, as a second-generation selective and irreversible EGFR family inhibitor, has demonstrated substantial clinical activity as a single agent in carcinomas (15–17). Recently, some studies reported that Afatinib had limited anti-tumor activity in CRPC patients (18), probably due to EGFR-targeted therapies desistance (19). Furthermore, in a phase II study, the CRPC patients showed no response to Gefitinib (another EGFR inhibitor), which showed a minimum anti-cancer activity (20). This resistance to gefitinib was perhaps due to an overactivity of the PI3K/Akt pathway in prostate cancer (21). On the contrary, the combination of EGFR inhibitors and other drugs is becoming a promising treatment for refractory prostate cancer. Inhibition of EGFR with cetuximab shows significantly improved PFS in prostate cancer patients with an overexpression of EGFR and persistent activity of PTEN (22). Thus, innovative treatment strategies are urgently needed for improving the survival of patients with prostate cancer.

Abnormal lipid metabolism plays an important role in the pathogenesis of prostate cancer. The cholesterol content of benign and cancerous human prostate glands' tissues were essentially double that of normal prostates (23). The urinary excretion of non-esterified cholesterol (NEC) is increased in metastatic prostate cancer (24). Liver X receptors (LXRs) are ligand-dependent nuclear receptor (NR) transcription factors, including LXR-α (NR1H3) and LXR-β (NR1H2), and have been well characterized as regulators of cholesterol homeostasis and lipogenesis (25). LXR-β is distributed ubiquitously, while LXR-α is expressed highly in metabolically active cells/tissues such as the liver, macrophages, and adipose tissue (26). LXR agonists, such as T0901317 and GW3965, can not only reduce intracellular cholesterol content (27), but also activate LXRs and inhibit the proliferation of cancer cells (28–31), including prostate cancer (32, 33). In addition to enhanced *de novo* cholesterol synthesis (34), the cholesterol absorption process is also regulated by EGFR signaling activity (35). Oncogenic transformation by EGFR increases the demand for cholesterol, and EGFR signaling antagonized LXR-α effects on cholesterol homeostasis (36). Furthermore, LXRs were significantly downregulated in tumor tissues and cells with an unknown mechanism (28, 33).

Herein, we demonstrate that LXR-α, but not LXR-β, shows lower levels in prostate cancer tissues than adjacent normal tissue. High expression of LXR-α in prostate cancer cells enhances the inhibition effects of LXR agonist GW3965 on cell proliferation and invasion. In addition, our study finds that LXR-α is regulated by the EGFR/AKT/FOXO3A axis and a combination of EGFR inhibitor Afatinib and GW3965 simultaneously increases and activates LXR-α, resulting in an increase of tumor suppressors and, ultimately, tumor inhibition. Therefore, our research will provide a theoretical basis for a new therapeutic treatment of progressive prostate cancer.

MATERIALS AND METHODS

Reagents and Cell Cultures

GW3965 (MCE, #HY-10627) and Afatinib (MCE, #HY-10261) were purchased from Selleck Chemicals, and dissolved in dimethyl sulfoxide (DMSO) (Amresco, #N182) and stored at −20°C. 22RV1, LNCaP, PC3, and DU145 cell lines were cultured at RPMI-1640 medium (Gibco, # 21870076). RWPE-1 cell line was grown in KSFM medium (Gibco, #10744019). All media were supplemented with 10% fetal bovine serum (FBS) and 1% penicillin-streptomycin. All the medium was purchased from Gibco. All cells were purchased from the Zhong Qiao Xin Zhou Biotechnology Co., Ltd. (Shanghai, China) and incubated at 37°C with 5% CO_2.

Cell Proliferation Assay

Cells were seeded into 96-well plates in triplicate. At different times after cell plating, cells were subjected to the Cell Counting Kit-8 (CCK-8) assay (MCE, HY-K0301), according to the manufacturer's instructions.

Immunoblotting (IB) and Antibodies

Western blot was performed as previously described (37). The following primary antibodies, which were purchased from Cell Signaling Technology, were used: Cleaved Caspase-3 (Asp175) (5A1E) (#9664), Cleaved Caspase-8 (Asp391) (18C8) (#9496), p21 (#2947), p27 (#3686), AKT (pan) (40D4) (#2920), Phospho-AKT (Ser473) (D9E) XP (#4060), and Bim (#2933). EGFR (#18986-1-AP), LXR-α (#14351-1-AP), LXR-β (#60345-1-Ig), CHOP (#15204-1-AP), FOXO3A (10849-1-AP), and GAPDH (#60004-1-Ig) were purchased from Proteintech. FLAG was obtained from Sigma-Aldrich (# F1804). All secondary antibodies were purchased from Cell Signaling Technology (Danvers, MA, United States).

Plate Colony-Forming Assay

Cells were seeded into 60-mm dishes in triplicate, followed by incubation at 37°C for 14–21 days. The colonies were then fixed with 4% paraformaldehyde, stained with crystal violet, and counted (38).

Lentivirus or Transient Transfection

For transient transfection, cells were seeded in antibiotic-free medium at 37°C for 24 h and transfected with FOXO3A siRNA or FOXO3A plasmid using lipofectamine-2000 transfection reagent (Life Technologies, Carlsbad, CA, United States) according to the manufacturer's instructions, and treated 48 h after transfection. The lentiviruses of LXR-α overexpression were purchased at GenePharma (Shanghai, China), and cells were transfected with lentivirus according to the manufacturer's protocol.

Transwell Migration Assay

Transwell assay was performed as described previously (39). The cells were cultured at 37°C in a humidified atmosphere with 5% CO_2 for 48 h. The cells below the sieve membrane were then fixed with 4% paraformaldehyde for 20 min and stained for 15 min with 0.5% crystal violet (Beyotime, China). The number of migrating cells in five fields were counted and the average number from each chamber was determined. Each experiment was conducted in triplicate.

Quantitative Real-Time PCR

Total RNA was isolated from prostate cells using RNAiso Plus (Takara, #9108), according to the manufacturer's instructions. Reverse transcription of the extracted RNA to corresponding complementary DNA was performed using PrimeScript RT reagent Kit with gDNA Eraser (Takara Bio, Inc., Otsu, Japan). RT-qPCR was performed with QuantiNovaTM SYBR® Green PCR Kit (Qiagen GmbH, Hilden, Germany) on an Applied Biosystems 7900HT Real-Time PCR System. The following forward (F) primers and reverse (R) primers were used: LXRα (sense, GGATAGGGTTGGAGT CAGCA; antisense, GGAGCGCCTGTTACACTGTT), LXRβ (sense, GCTCAGGAG CTGATGATCCA; antisense. GCGCTTGATCCTCGTG TAG), and GAPDH (sense, ATGG TGAAGGTCGGTGTG; antisense, ACCAGTGGATGC AGGGAT). The housekeeping gene, GAPDH, was used as loading controls. Each experiment was conducted in triplicate.

In vivo Xenograft Model

All animal experiments were carried out according to a protocol approved by the University Committee for Use and Care of Animals. Four- to six-week-old BALB/c athymic nude mice (nu/nu, female) were used with each experimental group, consisting of four mice. 2×10^6 PC3 cells were mixed 1:1 with matrigel (BD Biocoat #354230) in a total volume of 0.2 ml and then injected subcutaneously into the right flank side of nude mice, which were randomized into four groups and treated with vehicle, GW3965 (40 mg/kg/days, every day, per gavage), Afatinib (20 mg/kg/days, every day, per gavage) and GW3965 + Afatinib, when the tumor size reached about 100 mm^3. Mice were followed up for tumor size and body weight, and then killed after 21 days of treatment. Tumors were resected, weighed, and frozen or fixed in formalin and paraffin-embedded for immunohistochemical studies. The growth of tumors was measured twice a week and average tumor volume (TV) was calculated according to the equation: $TV = (L \times W^2)/2$.

Clinical Specimens

All four pair prostate samples (including tumor tissues and adjacent tissues) were derived from biopsy samples and were finally confirmed as prostate cancer with bone metastases. The study was conducted in accordance with the Declaration of Helsinki, and the protocol was approved by the Ethics Committee of the Army Medical University (Third Military Medical University) of China. Each patient had provided written informed consent prior to surgery.

Tissue Microarray

Tissue microarray was purchased from Servicebio (Wuhan, China), which provided chip information and completed immunohistochemical staining of the chips. IHC staining was performed on 34 paired samples (including 34 prostate tumor tissues and 34 paired adjacent tissues) for LXR detection. Furthermore, the above 34 prostate tumor tissues and another 25 prostate tumor tissues (totally 59 cases) were used to detect LXR and EGFR expression by IHC assay for further correlation analysis. The stained slides were observed under a microscope, and images were acquired and quantitatively classified based on staining intensity as described previously (40). Based on the staining intensity, we classified the samples into five groups: the weakest group (±), weak group (+), medium group (++), strong group (+++), and strongest group (++++). We defined the ±, +, and ++ groups as low-expression groups and the +++ and ++++ groups as high-expression groups.

Bioinformatics Analysis

Gene-Cloud Biotechnology information (GCBI)[1] is an online comprehensive bioinformatics analysis platform that predicts the regulation of genes and ncRNAs, transcription factors, and gene expression levels in disease. In the present study, GCBI was used to identify transcriptional regulators of LXR-α.

Statistical Analysis

All data were shown as the average ± standard deviation (Mean ± SD) and each experiment was repeated at least three times independently. All statistical analyses were performed using the GraphPad Prism Version 5.0 (San Diego, CA, United States). The statistical significance of differences between groups was examined by one-way analysis of variance (ANOVA) followed by Tukey's multiple comparison procedure or student's *t*-test. A *p*-value of less than 0.05 was considered statistically significant. Both CalcuSyn software and Jin's formula were used to evaluate the synergistic effects of drug combinations as described previously (41, 42).

RESULTS

LXRs Express in Prostate Cancer Cells and Tissues

To evaluate the expression of LXRs in prostate cancer tissue and normal tissue, we measured their expression status by immunoblotting (IB), immunohistochemistry (IHC), and q-PCR analysis. We selected 34 pairs of prostate cancer tissues and adjacent normal tissues from the tissue microarray. We found that LXR-α (**Figure 1A**), but not LXR-β (**Figure 1B**) protein level, was significantly reduced in prostate cancer tissues compared with adjacent normal tissues. We also collected 4 pairs of clinical samples (including tumor tissues and adjacent normal tissues) to detect the protein expression level of LXR-α and further confirmed that LXR-α protein level in prostate tumor tissue

[1] http://www.gcbi.com.cn/gclib/html/index

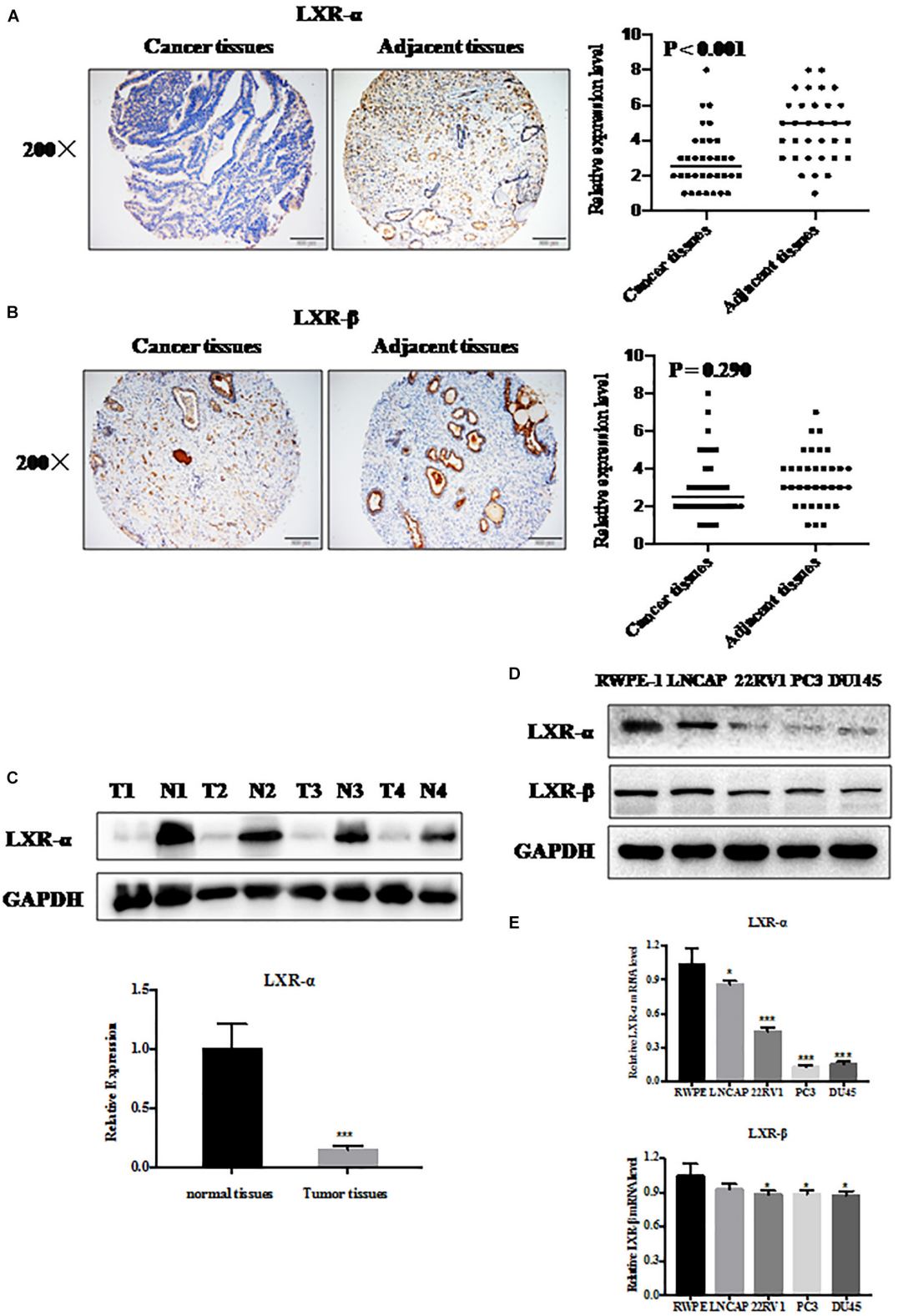

FIGURE 1 | LXR-α is down-regulated in prostate cancer cells and tissues. **(A,B)** LXR-α and LXR-β proteins expressed in prostate cancer tissues and adjacent tissues (n = 34) by immunohistochemistry (IHC). The microscope image was taken at ×200 magnification. **(C)** LXR-α protein levels in prostate cancer tissues and matched precancerous tissues were analyzed by IB analysis. **(D,E)** The levels of LXR-α and LXR-β in the prostate cells were analyzed by immunoblotting (IB) analysis. Data were presented as means ± SD. $^{*}p < 0.05$, $^{***}p < 0.001$, compared with the control group; n = 3. GAPDH levels served as the control for equal loading.

was lower than that in matching normal tissue (**Figure 1C**). Among LNCaP, 22RV1, PC3, and DU145 prostate cancer cell lines and one immortalized cell line (RWPE-1) tested, mRNA and protein levels of LXR-α were lower in prostate cancer cell lines (**Figures 1D,E**), whereas mRNA and protein levels of LXR-β were similar in all cell lines (**Figures 1D,E**).

LXR-α Inhibits Prostate Cancer Progression and Metastasis

To clarify the effect of LXRs on cell proliferation and metastasis of prostate cancer, we measured the levels of a few tumor suppressive and pro-apoptotic proteins upon LXRs overexpression. We found that overexpression of LXR-α induces the accumulation of multiple tumor suppressor proteins, including p21 and p27 (**Figure 2A**), which are known to regulate cell growth. Similarly, CHOP and Bim, as pro-apoptotic proteins, increased when LXR-α was overexpressed (**Figure 2A**). Compared to LXR-α overexpression, LXR-β overexpression had less influence on tumor suppressive and pro-apoptotic proteins (**Figure 2A**). Therefore, we selected LXR-α as the experimental subject. Next, we found that overexpression of LXR-α significantly inhibited cell growth (**Figure 2B**), clone-forming ability (**Figure 2C**)m and invasion ability (**Figure 2D**) of the PC3 cell line, suggesting that LXR-α was involved in prostate cancer progression and metastasis. LXRs are ligand-dependent receptors, thus, we next tested the effect of the GW3965 on the biological function of prostate cancer cells. GW3965 is a liver X receptor (LXR) agonist, which needs to be combined with LXR expression to exert its effect. The higher the expression level of LXR, the better the effect of GW3965. Compared with LXR-α transfected alone, co-treatment with GW3965 showed a better inhibition of cell proliferation (**Figure 2E**), colony-formation (**Figure 2F**), and invasion (**Figure 2G**) of the PC3 cell line with increased expression of p21, p27, E-cadherin, and C-Caspase 3, but decreased expression of N-cadherin (**Figure 2H**). These data suggested that a simultaneous increase of LXR-α can help to further inhibit progression and metastasis of prostate cancer.

LXR-α Is Regulated by EGFR/AKT/FOXO3 Pathway

We found that LXR-α expression is lower in prostate cancer cell lines and tissues (**Figure 1**). Meanwhile, EGFR was overexpressed and associated with poor prognosis in prostate cancer (43), and oncogenic transformation by EGFR increased the demand for cholesterol (36). Thus, we speculated that down-regulation of LXR-α might be mediated by EGFR. Next, we measured LXR-α and EGFR expression status in prostate cancer tissues by IHC staining. We selected 59 cancer tissues from the tissue microarray and found that the high EGFR staining group is largely associated with the low staining group of LXR-α ($p < 0.01$, $r = -0.424$), and vice versa (**Figure 3A**). To further elucidate how LXR-α is down-regulated in prostate cancer cells, a genetic bioinformatics database, the GCBI, was searched, which provides a web-lab with bioinformatics approaches to manage large amounts of transcriptome results. We found 54 potential transcription factors that may regulate LXR-α (**Figure 3B**), including FOXO3A (Forkhead box-containing protein class O3a). Some papers reported that FOXO3A is a transcriptional regulator, which can be regulated by EGFR (44–46). We therefore measured FOXO3A and EGFR expression in prostate cancer cell lines by IB. We found that FOXO3A is less expressed in high-grade malignant tumor cells and is negatively correlated with EGFR expression (**Figure 3C**). We speculated that down-regulation of LXR-α might be mediated by EGFR/FOXO3A. Consistently, EGFR inhibitor Afatinib decreased p-EGFR and p-AKT on PC3 and DU145 prostate cancer cell lines, in a dose-dependent manner (**Figure 3D**). Meanwhile, Afatinib increased FOXO3A protein as well as LXR-α protein (**Figure 3D**). Similarly, AKT inhibitor LY294002 increased FOXO3A and LXR-α protein in PC3 and DU145 cell lines (**Figure 3E**). We then determined whether down-regulation of LXR-α might be mediated by EGFR/AKT/FOXO3A. In a transfection experiment, the levels of endogenously expressed LXR-α were increased upon FOXO3A transfection (**Figure 3F**), while reduced by FOXO3A knockdown. Likewise, overexpression of FOXO3A elevated the level of LXR-α mRNA, and vice versa (**Figure 3G**), suggesting that FOXO3A regulated LXR-α by transcriptional control. Collectively, our results support that LXR-α is regulated by the EGFR/AKT/FOXO3A pathway.

Combination of GW3965 and Afatinib Shows Synergistic Lethality *in vitro*

We found that the EGFR inhibitor Afatinib could increase LXR-α levels (**Figure 3D**) and LXRs agonist GW3965 could activate LXR-α (**Figure 2**). Therefore, we supposed that a combination of GW3965 and Afatinib should have dual inhibition effects on prostate cancer cells by increasing and activating LXR-α. Both CalcuSyn software and Jin's formula were used as previously described to determine the synergy of the two agents. PC3 cell line was cultured with the combination of two drugs at different doses but in a constant ratio (GW3965 to Afatinib: 5–1.25 μM, 10–2.5 μM, and 20–5.0 μM, respectively) for 48 h. The combination of 5 μM GW3965 with 1.25 μM Afatinib in PC3 cell line inhibited cell proliferation by 28.0%, compared with monotherapy of GW3965 by 10.2% or Afatinib by 15.7%, indicating synergism (CI = 0.947; $Q = 0.94$; **Figure 4A**). Escalating doses, i.e., co-treatment with 10 μM GW3965 and 2.5 μM Afatinib (CI = 0.618; $Q = 1.18$) or 20 μM GW3965 and 5 μM Afatinib (CI = 0.538; $Q = 1.29$), showed synergetic effects in PC3 cell lines (**Figure 4A**). Furthermore, a combination of GW3965 with Afatinib significantly inhibited the clonogenic survival in the PC3 cell line (GW3965 or Afatinib vs. GW3965 + Afatinib: $P < 0.01$; **Figure 4B**), indicating that the combination of the two agents significantly inhibits cell proliferation or growth, which was further demonstrated by the increase of p27 (**Figure 4C**). In addition, the nature of suppression in cell proliferation or growth upon GW3965 and Afatinib combination was via induction of apoptosis (**Figure 4C**), as evidenced by the dose-dependent increased cleavage of caspase-3.

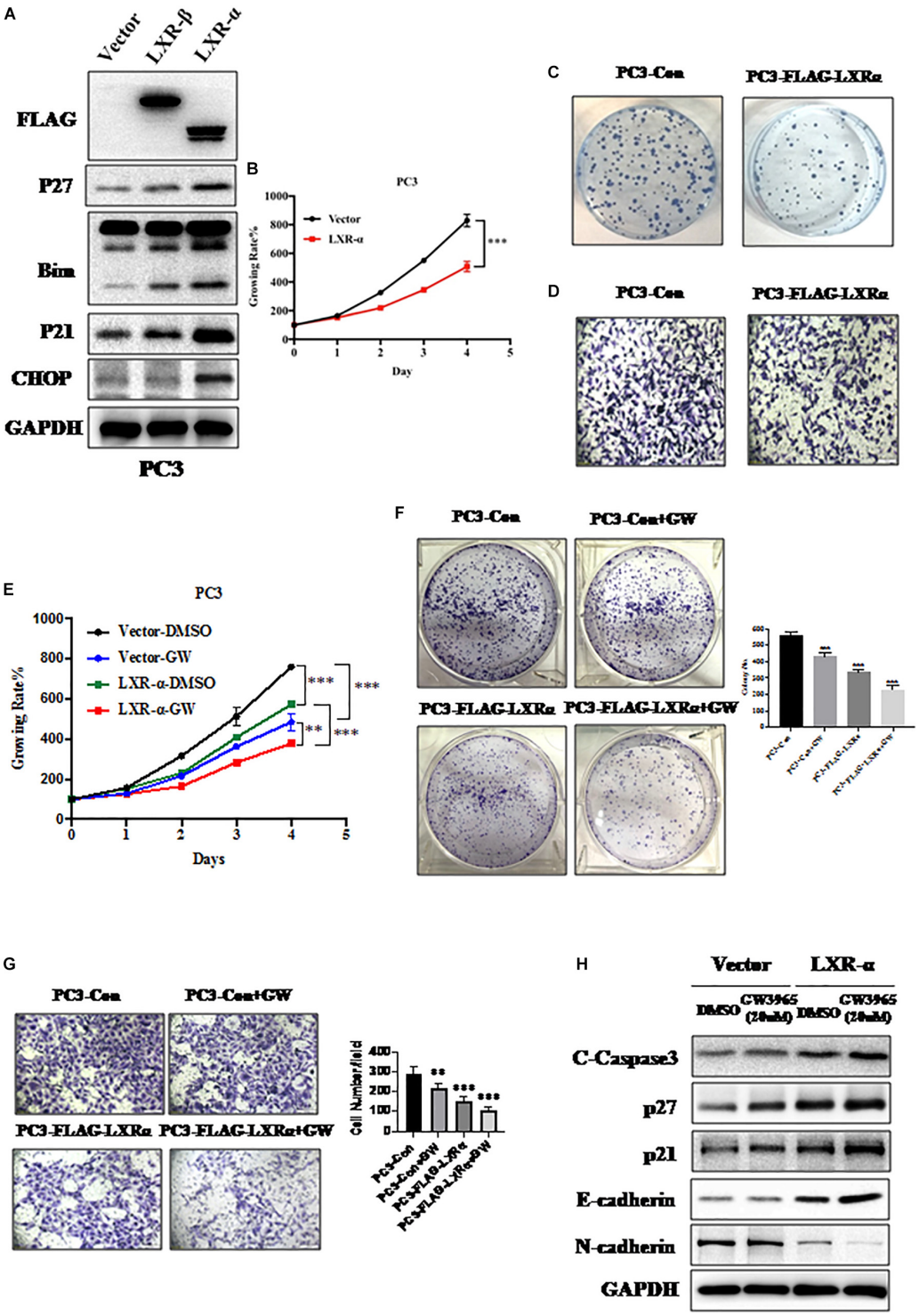

FIGURE 2 | Activation of LXR-α inhibits prostate cancer progression and metastasis. **(A)** Effects of LXRs' overexpression on the expression of cell progression-related protein in PC3 cell line. **(B)** Overexpression of LXR-α significantly inhibited cell proliferation in the PC3 cell line. Cell viability was detected with Cell Counting Kit-8 (CCK-8) assay. **(C)** Overexpression of LXR-α significantly suppressed colony formation in the PC3 cell line. **(D)** Overexpression of LXR-α extremely decreased cell invasion ability of the PC3 cell line. **(E)** Compared with LXR-α transfected alone, co-treatment with GW3965 could better inhibit cell proliferation. Cell viability was detected with CCK-8 assay. **(F)** Overexpression of LXR-α with concomitant treatment with GW3965 resulted in a greater inhibition of the clone-forming ability of PC3 cell line than GW3965 alone. **(G)** LXR-α overexpression decreased cell invasion ability of PC3 cell line, and did so more significantly through co-treatment with GW3965. **(H)** Compared with LXR-α transfected alone, co-treatment with GW3965 could better increase p21, p27, E-cadherin, and C-Caspase 3. Data were presented as means ± SD. $^{**}p < 0.01$, $^{***}p < 0.001$, compared with the control group; $n = 3$. GAPDH levels served as the control for equal loading.

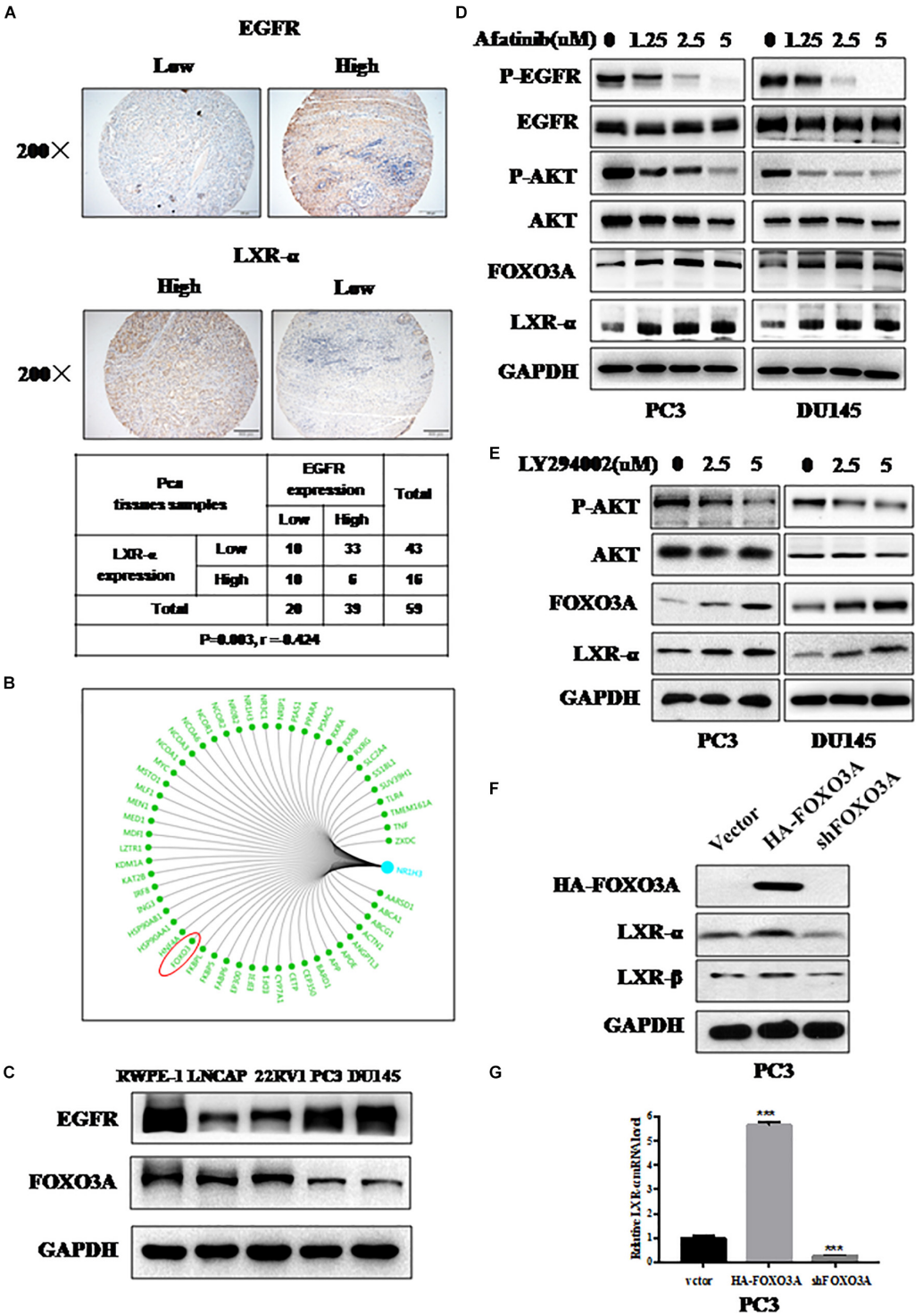

Pca tissues samples		EGFR expression		Total
		Low	High	
LXR-α expression	Low	10	33	43
	High	10	6	16
Total		20	39	59
P=0.003, r =-0.424				

FIGURE 3 | LXR-α is regulated by EGFR/AKT/FOXO3 pathway. **(A)** LXR-α and EGFR protein expressed in prostate cancer (n = 59) by IHC. The microscope image was taken at ×200 magnification. **(B)** Bioinformatics analysis comes from https://www.gcbi.com.cn/gclib/html/index. **(C)** Basal level of FOXO3A and EGFR protein in prostate cell lines. **(D)** EGFR inhibitor Afatinib dose-dependently increased FOXO3A and LXR-α levels in PC3 and DU145 cell lines. Prostate cancer cell lines were treated with different doses of Afatinib for 48 h, followed by determination of related-protein expression using IB analysis. **(E)** AKT inhibitor LY294002 dose-dependently increased FOXO3A and LXR-α levels in PC3 and DU145 cell lines. Prostate cancer cell lines were treated with different doses of LY294002 for 48 h, followed by determination of related-protein expression using IB analysis. **(F)** In a transfection experiment, the levels of endogenously expressed LXR-α were increased upon FOXO3A transfection, while they were reduced by FOXO3A knockdown. **(G)** Overexpression of FOXO3A elevated the level of LXR-α mRNA, while they were reduced by FOXO3A knockdown. Data were presented as means ± SD. ***$p < 0.001$, compared with the control group; n = 3. GAPDH levels served as the control for equal loading.

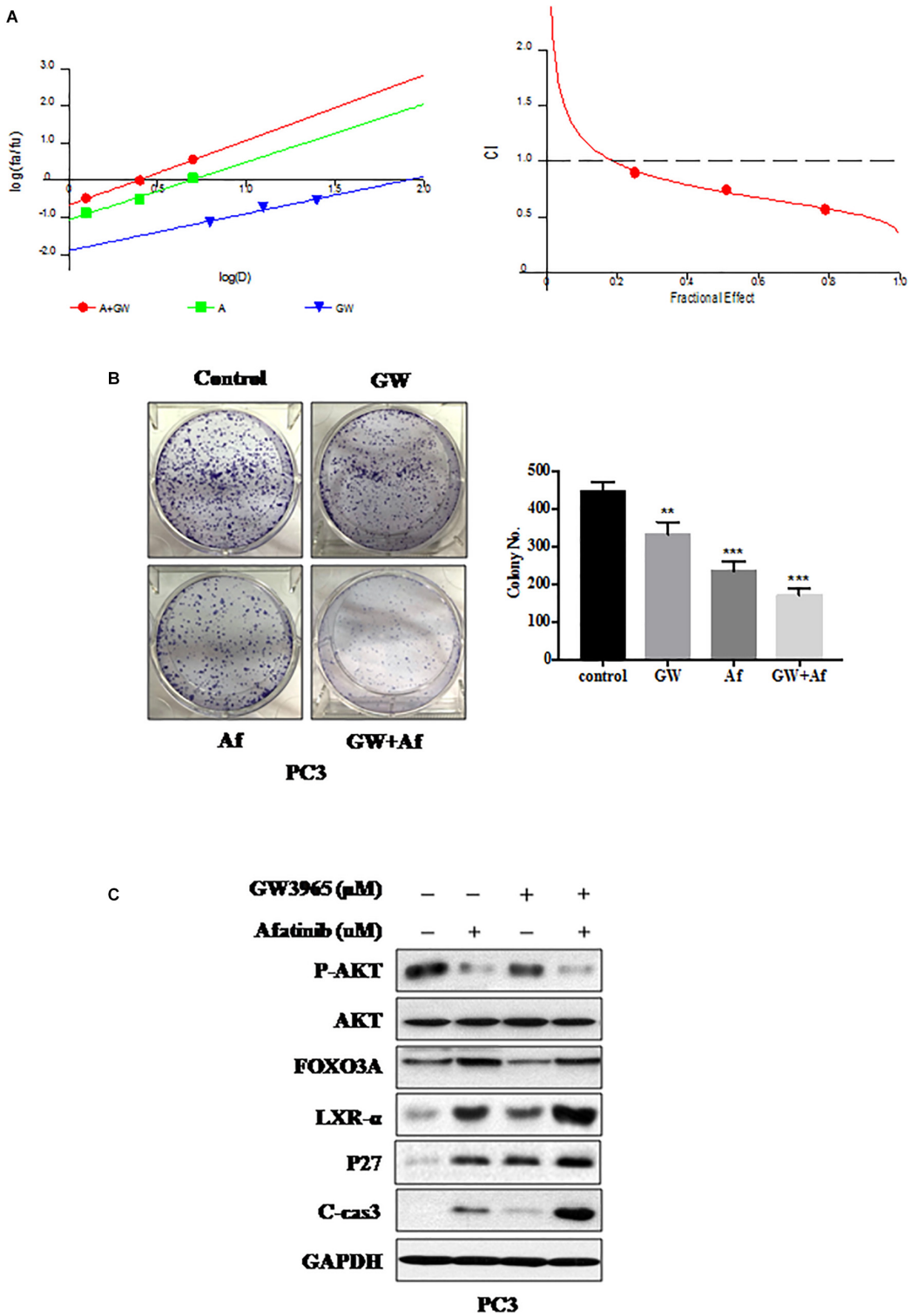

FIGURE 4 | Combination of GW3965 and Afatinib shows synergistic lethality *in vitro*. **(A)** GW3965 and Afatinib showed synergistic effects in PC3 cell line. CI-effect plots and median effect plots were generated using CalcuSyn software. The points a, b, and c represent CI values for the combinations 5, 10, and 20 μM GW3965 with 1.25, 2.5, and 5 μM Afatinib in a constant ratio, respectively. **(B)** Combination of GW3965 and Afatinib inhibits cell colony formation in prostate cancer cells. PC3 cell line was treated with GW3965 (10 μM) or Afatinib (2.5 μM) alone or with a combination of the two compounds, followed by the colorogenic assay. The data were expressed as mean ± S.D. (**$p < 0.01$, ***$p < 0.001$; Student's *t*-test) compared with control groups. **(C)** Combination of GW3965 and Afatinib simultaneously increased and activated LXR-α in the PC3 cell line. PC3 cell line was examined after 48 h of treatment with DMSO, 10 μM GW3965, and/or 2.5 μM Afatinib, and determined the related protein expression by IB analysis.

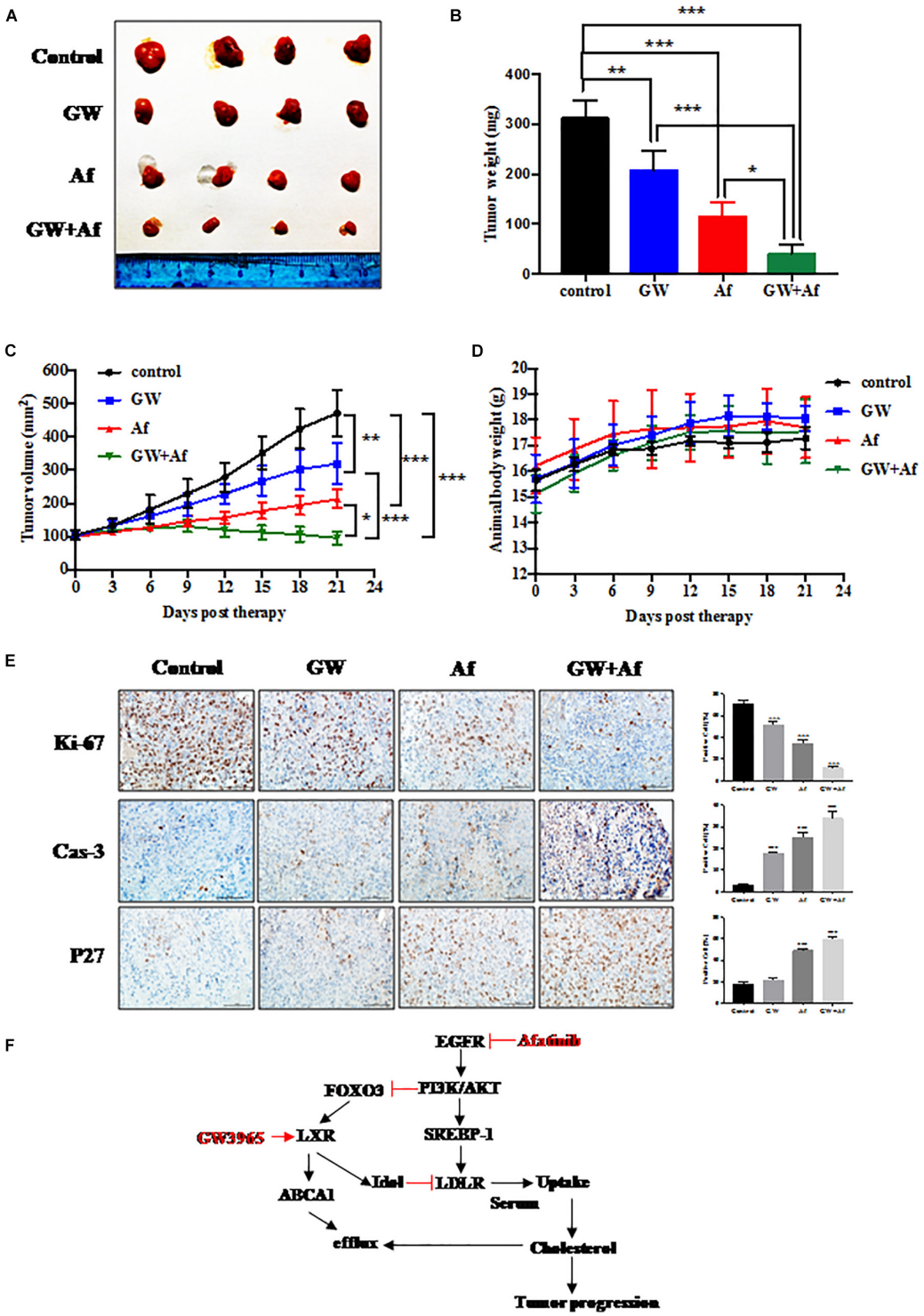

FIGURE 5 | Combination of GW3965 and Afatinib shows synergistic lethality *in vivo*. **(A–E)** Synergistic anti-tumor activity of GW3965 and Afatinib in the PC3 xenograft model. PC3 cell line was injected subcutaneously into the right flank side of nude mice. The mice were randomized when the tumor size reached about 100 mm^3 and were treated as follows: vehicle, $n = 4$; GW3965 (40 mg/kg/days for every day for 4 weeks), $n = 4$; Afatinib (20 mg/kg/days for every day for 4 weeks), $n = 4$; GW3965 + Afatinib, $n = 5$. The tumor growth was monitored and growth curve was plotted **(C)** and tumors were harvested **(A)** and weighted **(B)**. Body weight was measured during the treatment and plotted **(D)**. Schematic model depicting the mechanisms of action underlying nobiletin-induced anti-proliferation. **(E)** Immunohistochemical staining of xenograft tumor tissues. Tumor tissues from four groups of mice were fixed, sectioned, and stained with indicated antibodies. Scale bars: 100 μm. Shown are mean ± SEM, $^*p < 0.05$; $^{**}p < 0.01$, $^{***}p < 0.001$. **(F)** Schematic model depicting the mechanisms of action underlying LXR-α inhibited prostate cancer progression, which was regulated by EGFR/AKT/FOXO3 pathway.

Combination of GW3965 and Afatinib Shows Synergistic Lethality *in vivo*

We next validated the above *in vitro* findings by using an *in vivo* xenograft model. PC3 xenograft model was established and treated with vehicle, GW3965, and/or Afatinib. Consistent with the *in vitro* results, the combination of GW3965 and Afatinib suppressed tumor growth significantly more than single-agent treatment (**Figure 5A**). Consistently, the average tumor size and tumor weight at the end of experiment (treatment with 21 days) were significantly lower in the combination GW3965 and Afatinib group (**Figures 5B,C**). Body weight of the xenograft model was unchanged during drug treatment, suggesting that the effect on normal tissues was minimal (**Figure 5D**). Importantly, IHC staining of tumor tissues revealed that, compared with GW3965 or Afatinib single-agent treatment, a combination of the two agents more significantly inhibited cell growth (decrease of Ki-67 and increase of p27) and induced apoptosis (increase of cleavage caspase-3) (GW3965 or Afatinib vs. GW3965 + Afatinib: $P < 0.01$; **Figure 5E**). Collectively, the combination of GW3965 with Afatinib more significantly inhibited prostate cell growth and survival than single-agent treatment, with less effect on normal tissues.

DISCUSSION

Liver X receptors, including LXR-α and LXR-β, are ligand-dependent nuclear receptors, which have more anti-proliferative effects on a variety of cancer cells (28–31). Our results demonstrated that LXR-α had more anti-proliferative effects on prostate cancer cell lines than LXR-β (**Figures 1**, **2**). We also revealed a positive correlation between lower LXR-α levels and high-grade malignancy prostate cancer cell lines, and vice versa (**Figures 1D,E**). LXR-α has been implicated in growth regulation of a variety of cancer cells (28, 47, 48), but the regulation of prostate cancer cell growth has never been previously reported. Herein, we showed that LXR-α acts as a tumor suppressor in prostate cancer with the following lines of supporting evidence: (1) LXR-α is down-regulated in prostate cancer tissues and high levels of LXR-α predicts a biomarker for prostate cancer; (2) Overexpression of LXR-α significantly inhibits the growth and metastasis of prostate cancer cells; and (3) The tumor suppressor function of LXR-α is mediated by the accumulation of the bona fide tumor suppressors, including p21 and p27. Some papers reported activation of LXRs could increase p21 and p27 (32, 33, 49). LXR agonists have been developed as potential drugs for the treatment of cardiovascular diseases and metabolic syndromes (50, 51), which are potential targets in cancer prevention and treatment. Previous studies demonstrated that LXR agonist T0901317 inhibited prostate cancer cell growth (32, 33), while our results further demonstrated the LXR agonist GW3965 can inhibit growth and metastasis of prostate cancer cells (**Figure 2**).

Although LXR-α inhibits cancer cell growth, the underlying mechanisms of this have never been previously reported. We found, for the first time, that LXR-α is regulated by the EGFR/AKT/FOXO3A pathway. Our conclusion is supported by the following lines of evidence: (1) Among 59 tumor TMA samples, the high EGFR staining group is largely associated with the low staining group of LXR-α, and vice versa; (2) Among prostate cell lines tested, there is a general tendency of inversed protein levels between EGFR and FOXO3A. FOXO3A could induce cholesterol regulation and lipid management (52), and be regulated by EGFR (44–46); (3) EGFR inhibitor Afatinib inhibited p-AKT and increased FOXO3A and LXR-α, as did AKT inhibitor LY294002; (4) The levels of endogenously expressed LXR-α were increased upon FOXO3A transfection, while they were reduced by FOXO3A knockdown; and (5) Overexpression of FOXO3A elevated the level of LXR-α mRNA, and vice versa.

Afatinib shows potent activity against wild-type and mutant forms of EGFR (53–56). However, patients who initially benefit from EGFR-targeted therapies eventually develop resistance (19). Afatinib had limited anti-tumor activity in unselected advanced CRPC patients (18). Thus, innovative treatment strategies are urgently needed for improving the survival of patients with prostate cancer. We found a combination of GW3965 and Afatinib simultaneously increased and activated LXR-α, which led to increased expression levels of tumor suppressor p27, eventually inhibiting tumor formation. Recently, it was shown that EGFR inhibitor synergized with LXRα agonists in killing cancer cells (36); for example, LXR ligands combined with gefitinib could better suppress cell cycle progression in NSCLC cells (57, 58). Therefore, a combination of LXR agonist GW3965 and Afatinib may serve as a potential therapeutic strategy for prostate cancer.

Our study also raised a question. It is well known that EGFR/PI3K/Akt signaling regulates LDLR mediated by SREBP-1, thereby promoting cell uptake of cholesterol from serum (35). Herein, we only confirmed that the EGFR/AKT signaling pathway can also down-regulate the expression of LXR-α by inhibiting the expression of the transcription factor FOXO3A. We will continue to pursue whether EGFR disturbs cancer cell cholesterol homeostasis by down-regulating cholesterol efflux through this new signal pathway, so as to have a more comprehensive understanding of the effect of EGFR on the metabolism of cholesterol in cancer cells.

CONCLUSION

In conclusion, we reveal that the protein level of LXR-α, but not LXR-β, is higher in prostate cancer tissues than adjacent normal tissues. Moreover, we find that LXR-α is regulated by the EGFR/AKT/FOXO3A pathway. Afatinib, an EGFR inhibitor, down-regulates the activity of PI3K/AKT signaling pathway by inhibiting EGFR, thereby promoting the expression of FOXO3A. FOXO3A as a transcription factor further up-regulates the expression of LXR-α. GW3965 is a liver X receptor (LXR) agonist, which needs to be combined with LXR to exert its effect. Therefore, we further confirm that a combination of Afatinib and GW3965 simultaneously increases and activates LXR-α, resulting in an increase of tumor suppressors and, ultimately, tumor inhibition (**Figure 5F**). Above all, this combination therapy

may become a potential treatment strategy for prostate cancer, especially progressive prostate cancer.

DATA AVAILABILITY STATEMENT

The raw data supporting the conclusions of this article will be made available by the authors, without undue reservation.

ETHICS STATEMENT

The studies involving human participants were reviewed and approved by Ethics Committee of the Army Medical University (Third Military Medical University) of China. The patients/participants provided their written informed consent to participate in this study. The animal study was reviewed and approved by the Institutional Animal Care and Use Committee of Model Animal Research Center of Army Medical University (Third Military Medical University) of China.

AUTHOR CONTRIBUTIONS

WF and JX did the conception and design of the research, and edited and revised the manuscript. TC performed the experiments, interpreted the results of the experiments, and prepared the figures. TC and WF drafted the manuscript. All authors read and approved the final manuscript.

FUNDING

This work was supported by the National Natural Science Foundation of China (Grant No. 81772702 to JX and Grant No. 81502214 to WF).

REFERENCES

1. Turkbey B, Brown AM, Sankineni S, Wood BJ, Pinto PA, Choyke PL. Multiparametric prostate magnetic resonance imaging in the evaluation of prostate cancer. *CA Cancer J Clin.* (2016) 66:326–36. doi: 10.3322/caac.21333
2. Chen W, Zheng R, Baade PD, Zhang S, Zeng H, Bray F, et al. Cancer statistics in China, 2015. *CA Cancer J Clin.* (2016) 66:115–32. doi: 10.3322/caac.21338
3. Chen W, Zheng R, Zhang S, Zeng H, Zuo T, Xia C, et al. Cancer incidence and mortality in China in 2013: an analysis based on urbanization level. *Chin J Cancer Res.* (2017) 29:1–10. doi: 10.21147/j.issn.1000-9604.2017.01.01
4. Dehm SM, Tindall DJ. Molecular regulation of androgen action in prostate cancer. *J Cell Biochem.* (2006) 99:333–44. doi: 10.1002/jcb.20794
5. Hellerstedt BA, Pienta KJ. The current state of hormonal therapy for prostate cancer. *CA Cancer J Clin.* (2002) 52:154–79. doi: 10.3322/canjclin.52.3.154
6. Santer FR, Erb HH, McNeill RV. Therapy escape mechanisms in the malignant prostate. *Semin Cancer Biol.* (2015) 35:133–44. doi: 10.1016/j.semcancer.2015.08.005
7. Ettinger SL, Sobel R, Whitmore TG, Akbari M, Bradley DR, Gleave ME, et al. Dysregulation of sterol response element-binding proteins and downstream effectors in prostate cancer during progression to androgen independence. *Cancer Res.* (2004) 64:2212–21. doi: 10.1158/0008-5472.can-2148-2
8. Harris WP, Mostaghel EA, Nelson PS, Montgomery B. Androgen deprivation therapy: progress in understanding mechanisms of resistance and optimizing androgen depletion. *Nat Clin Pract Urol.* (2009) 6:76–85. doi: 10.1038/ncpuro1296
9. Traish AM, Morgentaler A. Epidermal growth factor receptor expression escapes androgen regulation in prostate cancer: a potential molecular switch for tumour growth. *Br J Cancer.* (2009) 101:1949–56. doi: 10.1038/sj.bjc.6605376
10. Kambhampati S, Ray G, Sengupta K, Reddy VP, Banerjee SK, Van Veldhuizen PJ. Growth factors involved in prostate carcinogenesis. *Front Biosci.* (2005) 10:1355–67. doi: 10.2741/1625
11. Wee P, Wang Z. Epidermal growth factor receptor cell proliferation signaling pathways. *Cancers (Basel).* (2017) 9:52. doi: 10.3390/cancers9050052
12. Chang YS, Chen WY, Yin JJ, Sheppard-Tillman H, Huang J, Liu YN. EGF receptor promotes prostate cancer bone metastasis by downregulating miR-1 and activating TWIST1. *Cancer Res.* (2015) 75:3077–86. doi: 10.1158/0008-5472.CAN-14-3380
13. Lin HP, Ho HM, Chang CW, Yeh SD, Su YW, Tan TH, et al. DUSP22 suppresses prostate cancer proliferation by targeting the EGFR-AR axis. *FASEB J.* (2019) 33:14653–67. doi: 10.1096/fj.201802558RR
14. Zhau HE, Wan DS, Zhou J, Miller GJ, von Eschenbach AC. Expression of c-erb B-2/neu proto-oncogene in human prostatic cancer tissues and cell lines. *Mol Carcinog.* (1992) 5:320–7. doi: 10.1002/mc.2940050413
15. Yang JC, Wu YL, Schuler M, Sebastian M, Popat S, Yamamoto N, et al. Afatinib versus cisplatin-based chemotherapy for EGFR mutation-positive lung adenocarcinoma (LUX-Lung 3 and LUX-Lung 6): analysis of overall survival data from two randomised, phase 3 trials. *Lancet Oncol.* (2015) 16:141–51. doi: 10.1016/S1470-2045(14)71173-8
16. Chen Q, Huang Y, Shao L, Han-Zhang H, Yang F, Wang Y, et al. An EGFR-amplified cervical squamous cell carcinoma patient with pulmonary metastasis benefits from afatinib: a case report. *Onco Targets Ther.* (2020) 13:1845–9. doi: 10.2147/OTT.S236382
17. Starrett JH, Guernet AA, Cuomo ME, Poels KE, van Alderwerelt van Rosenburgh IK, Nagelberg A, et al. Drug sensitivity and allele-specificity of first-line osimertinib resistance EGFR mutations. *Cancer Res.* (2020) 34:1. doi: 10.1158/0008-5472.CAN-19-3819
18. Molife LR, Omlin A, Jones RJ, Karavasilis V, Bloomfield D, Lumsden G, et al. Randomized Phase II trial of nintedanib, afatinib and sequential combination in castration-resistant prostate cancer. *Future Oncol.* (2014) 10:219–31. doi: 10.2217/fon.13.250
19. Chong CR, Janne PA. The quest to overcome resistance to EGFR-targeted therapies in cancer. *Nat Med.* (2013) 19:1389–400. doi: 10.1038/nm.3388
20. Canil CM, Moore MJ, Winquist E, Baetz T, Pollak M, Chi KN, et al. Randomized phase II study of two doses of gefitinib in hormone-refractory prostate cancer: a trial of the National Cancer Institute of Canada-clinical trials group. *J Clin Oncol.* (2005) 23:455–60. doi: 10.1200/JCO.2005.02.129
21. She QB, Solit D, Basso A, Moasser MM. Resistance to gefitinib in PTEN-null HER-overexpressing tumor cells can be overcome through restoration of PTEN function or pharmacologic modulation of constitutive phosphatidylinositol 3'-kinase/Akt pathway signaling. *Clin Cancer Res.* (2003) 9:4340–6.
22. Cathomas R, Rothermundt C, Klingbiel D, Bubendorf L, Jaggi R, Betticher DC, et al. Efficacy of cetuximab in metastatic castration-resistant prostate cancer might depend on EGFR and PTEN expression: results from a phase II trial (SAKK 08/07). *Clin Cancer Res.* (2012) 18:6049–57. doi: 10.1158/1078-0432.CCR-12-2219
23. Sporer A, Brill DR, Schaffner CP. Epoxycholesterols in secretions and tissues of normal, benign, and cancerous human prostate glands. *Urology.* (1982) 20:244–50. doi: 10.1016/0090-4295(82)90631-8
24. Acevedo HF, Campbell EA, Saier EL, Frich JC Jr., Merkow LP, Hayeslip DW, et al. Urinary cholesterol. V. Its excretion in men with testicular and prostatic neoplasms. *Cancer.* (1973) 32:196–205. doi: 10.1002/1097-0142(197307)32:13.0.co;2-6
25. Zhao C, Dahlman-Wright K. Liver X receptor in cholesterol metabolism. *J Endocrinol.* (2010) 204:233–40. doi: 10.1677/JOE-09-0271
26. Bischoff ED, Daige CL, Petrowski M, Dedman H, Pattison J, Juliano J, et al. Non-redundant roles for LXRalpha and LXRbeta in atherosclerosis

susceptibility in low density lipoprotein receptor knockout mice. *J Lipid Res.* (2010) 51:900–6. doi: 10.1194/jlr.M900096
27. Wu G, Wang Q, Xu Y, Li J, Zhang H, Qi G, et al. Targeting the transcription factor receptor LXR to treat clear cell renal cell carcinoma: agonist or inverse agonist? *Cell Death Dis.* (2019) 10:416. doi: 10.1038/s41419-019-1654-6
28. Liang X, Cao Y, Xiang S, Xiang Z. LXRalpha-mediated downregulation of EGFR suppress colorectal cancer cell proliferation. *J Cell Biochem.* (2019) 120:17391–404. doi: 10.1002/jcb.29003
29. Nguyen-Vu T, Vedin LL, Liu K, Jonsson P, Lin JZ, Candelaria NR, et al. Liver x receptor ligands disrupt breast cancer cell proliferation through an E2F-mediated mechanism. *Breast Cancer Res.* (2013) 15:R51. doi: 10.1186/bcr3443
30. Pencheva N, Buss CG, Posada J, Merghoub T, Tavazoie SF. Broad-spectrum therapeutic suppression of metastatic melanoma through nuclear hormone receptor activation. *Cell.* (2014) 156:986–1001. doi: 10.1016/j.cell.2014.01.038
31. Lee CS, Park M, Han J, Lee JH, Bae IH, Choi H, et al. Liver X receptor activation inhibits melanogenesis through the acceleration of ERK-mediated MITF degradation. *J Invest Dermatol.* (2013) 133:1063–71. doi: 10.1038/jid.2012.409
32. Fukuchi J, Kokontis JM, Hiipakka RA, Chuu CP, Liao S. Antiproliferative effect of liver X receptor agonists on LNCaP human prostate cancer cells. *Cancer Res.* (2004) 64:7686–9. doi: 10.1158/0008-5472.CAN-04-2332
33. Chuu CP, Lin HP. Antiproliferative effect of LXR agonists T0901317 and 22(R)-hydroxycholesterol on multiple human cancer cell lines. *Anticancer Res.* (2010) 30:3643–8.
34. Silvente-Poirot S, Poirot M. Cancer. Cholesterol and cancer, in the balance. *Science.* (2014) 343:1445–6. doi: 10.1126/science.1252787
35. Guo D, Reinitz F, Youssef M, Hong C, Nathanson D, Akhavan D, et al. An LXR agonist promotes glioblastoma cell death through inhibition of an EGFR/AKT/SREBP-1/LDLR-dependent pathway. *Cancer Discov.* (2011) 1:442–56. doi: 10.1158/2159-8290.CD-11-0102
36. Gabitova L, Restifo D, Gorin A, Manocha K, Handorf E, Yang DH, et al. Endogenous sterol metabolites regulate growth of EGFR/KRAS-dependent tumors via LXR. *Cell Rep.* (2015) 12:1927–38. doi: 10.1016/j.celrep.2015.08.023
37. Xu J, Yue CF, Zhou WH, Qian YM, Zhang Y, Wang SW, et al. Aurora-A contributes to cisplatin resistance and lymphatic metastasis in non-small cell lung cancer and predicts poor prognosis. *J Transl Med.* (2014) 12:200. doi: 10.1186/1479-5876-12-200
38. Zhou W, Xu J, Li H, Xu M, Chen ZJ, Wei W, et al. Neddylation E2 UBE2F promotes the survival of lung cancer cells by activating CRL5 to degrade NOXA via the K11 linkage. *Clin Cancer Res.* (2017) 23:1104–16. doi: 10.1158/1078-0432.CCR-16-1585
39. Xu J, Wu X, Zhou WH, Liu AW, Wu JB, Deng JY, et al. Aurora-A identifies early recurrence and poor prognosis and promises a potential therapeutic target in triple negative breast cancer. *PLoS One.* (2013) 8:e56919. doi: 10.1371/journal.pone.0056919
40. Li L, Zhang W, Liu Y, Liu X, Cai L, Kang J, et al. The CRL3(BTBD9) E3 ubiquitin ligase complex targets TNFAIP1 for degradation to suppress cancer cell migration. *Signal Transduct Target Ther.* (2020) 5:42. doi: 10.1038/s41392-020-0140-z
41. Jin ZJ. Addition in drug combination. *Acta Pharmacol Sin.* (1980) 1:70–6.
42. Chou TC. Theoretical basis, experimental design, and computerized simulation of synergism and antagonism in drug-combination studies (vol 58, pg 621, 2006). *Pharmacol Rev.* (2007) 59:124.
43. Baek KH, Hong ME, Jung YY, Lee CH, Lee TJ, Park ES, et al. Correlation of AR, EGFR, and HER2 expression levels in prostate cancer: immunohistochemical analysis and chromogenic In Situ hybridization. *Cancer Res Treat.* (2012) 44:50–6. doi: 10.4143/crt.2012.44.1.50
44. Wu WR, Lin JT, Pan CT, Chan TC, Liu CL, Wu WJ, et al. Amplification-driven BCL6-suppressed cytostasis is mediated by transrepression of FOXO3 and post-translational modifications of FOXO3 in urinary bladder urothelial carcinoma. *Theranostics.* (2020) 10:707–24. doi: 10.7150/thno.39018
45. Yao YL, Zhou LS, Liao WF, Chen HJ, Du ZY, Shao CH, et al. HH1-1, a novel Galectin-3 inhibitor, exerts anti-pancreatic cancer activity by blocking Galectin-3/EGFR/AKT/FOXO3 signaling pathway. *Carbohydrate Polymers.* (2019) 204:111–23. doi: 10.1016/j.carbpol.2018.10.008
46. Qi WT, Weber CR, Wasland K, Roy H, Wali R, Joshi S, et al. Tumor suppressor FOXO3 mediates signals from the EGF receptor to regulate proliferation of colonic cells. *Am J Physiol Gastrointestinal Liver Physiol.* (2011) 300:G264–72. doi: 10.1152/ajpgi.00416.2010
47. Hu C, Liu D, Zhang Y, Lou G, Huang G, Chen B, et al. LXR alpha-mediated downregulation of FOXM1 suppresses the proliferation of hepatocellular carcinoma cells. *Oncogene.* (2014) 33:2888–97. doi: 10.1038/onc.2013.250
48. Chang YW, Zhao YF, Cao YL, Gu XF, Li ZQ, Wang SQ, et al. Liver X receptor alpha inhibits osteosarcoma cell proliferation through up-regulation of FoxO1. *Cell Physiol Biochem.* (2013) 32:180–6. doi: 10.1159/000350134
49. Rough JJ, Monroy MA, Yerrum S, Daly JM. Anti-proliferative effect of LXR agonist T0901317 in ovarian carcinoma cells. *J Ovarian Res.* (2010) 3:13. doi: 10.1186/1757-2215-3-13
50. Chuu CP, Kokontis JM, Hiipakka RA, Liao SS. Modulation of liver X receptor signaling as novel therapy for prostate cancer. *J Biomed Sci.* (2007) 14:543–53. doi: 10.1007/s11373-007-9160-8
51. Peng DC, Hiipakka RA, Dai Q, Guo J, Reardon CA, Getz GS, et al. Antiatherosclerotic effects of a novel synthetic tissue-selective steroidal liver X receptor agonist in low-density lipoprotein receptor-deficient mice. *J Pharmacol Exp Ther.* (2008) 327:332–42. doi: 10.1124/jpet.108.142687
52. Gao WY, Chen PY, Chen SF, Wu MJ, Chang HY, Yen JH. Pinostrobin inhibits proprotein convertase subtilisin/kexin-type 9 (PCSK9) gene expression through the modulation of FoxO3a protein in HepG2 cells. *J Agric Food Chem.* (2018) 66:6083–93. doi: 10.1021/acs.jafc.8b02559
53. Yang X, Huang C, Chen R, Zhao J. Resolving resistance to osimertinib therapy with afatinib in an NSCLC patient with EGFR L718Q mutation. *Clin Lung Cancer.* (2020) 21:e258–60. doi: 10.1016/j.cllc.2019.12.002
54. Passaro A, Laktionov KK, Poltoratskiy A, Egorova I, Hochmair M, Migliorino MR, et al. Afatinib in EGFR TKI-naive patients (pts) with locally advanced/metastatic NSCLC harbouring EGFR mutations: an interim analysis of a phase IIIB trial. *Ann Oncol.* (2019) 30:ii38–68.
55. Yang JC, Schuler M, Popat S, Miura S, Heeke S, Park K, et al. Afatinib for the treatment of NSCLC harboring uncommon EGFR mutations: a database of 693 cases. *J Thorac Oncol.* (2020) 15:803–15. doi: 10.1016/j.jtho.2019.12.126
56. Zhang ZH, Zeng KM, Zhao S, Zhao YY, Hou X, Luo F, et al. Pemetrexed/carboplatin plus gefitinib as a first-line treatment for EGFR-mutant advanced nonsmall cell lung cancer: a Bayesian network meta-analysis. *Ther Adv Med Oncol.* (2019) 11:1758835919891652. doi: 10.1177/1758835919891652
57. Wairagu PM, Park KH, Kim J, Choi JW, Kim HW, Yeh BI, et al. Combined therapeutic potential of nuclear receptors with receptor tyrosine kinase inhibitors in lung cancer. *Biochem Biophys Res Commun.* (2014) 447:490–5. doi: 10.1016/j.bbrc.2014.04.018
58. Liu SW, Cao HX, Chen D, Yu SR, Sha HH, Wu JZ, et al. LXR ligands induce apoptosis of EGFR-TKI-resistant human lung cancer cells in vitro by inhibiting Akt-NF-kappa B activation. *Oncol Lett.* (2018) 15:7168–74. doi: 10.3892/ol.2018.8182

Conflict of Interest: The authors declare that the research was conducted in the absence of any commercial or financial relationships that could be construed as a potential conflict of interest.